Enhancing Grinding Precision: Machine Vision Analysis for Predicting Titanium Alloy (Gr5) Surface Texture

Dr.M. Prithiviraj[1], D. Palanikumar[1], A.Sankara Narayana murthy[1], S.Muthunatarajan[1], K.Murugananthan[1]

[1]Department of Mechanical Engineering, Faculty Kamaraj college of Engineering and technology, Virudhunagar, Tamil Nadu, 626005, India

Abstract

Surface finish of parts significantly enriches its look and total value. Surface inspection plays a vital role in the control of product quality. Bulks of commercially available surface roughness evaluating gadgets are of contact type and are broadly acknowledged for examination. But these contact type instruments are incompetent for speedier assessment and incompatible for automation. The computer vision systems are of non-contact type and are capable of making image analysis easier and flexible. Taguchi's mixed level parameter design (L27) is used for the experimental design. Cutting speed, feed rate and depth of cut are considered as machining parameters. Regression analysis is applied to predict the surface roughness of the ground surfaces of titanium alloy. In this research work, images of the ground surfaces of titanium alloy are captured using a CCD camera and these digital images are subsequently, magnified using Cubic Convolution, Nearest Neighbor and Bilinear interpolation techniques. Then, the optical surface roughness parameter G_a is evaluated for the captured original images and magnified better-quality images. A good correlation between magnification factor, estimated G_a and surface standard values with higher correlation coefficient is achieved.

Keywords: *Magnification factor, Interpolation algorithms, Surface roughness, Aerospace titanium alloy(gr5), Machine vision, Orthogonal array.*

1. Introduction

Aviation, automotive, nuclear, marine, biomedical, petroleum refining and chemical processing industries use titanium alloy largely in recent manufacturing processes because of light weight with high strength, extraordinary corrosion resistance and the ability to withstand extreme temperatures. Ti-6Al-4V or Grade 5 titanium is identified as the "workhorse" of the titanium alloys because of its combination of toughness and strength. It represents 50 percent of aggregate titanium utilization the world over. Titanium is by and large used for parts requesting the most extreme consistency and hence the surface integrity must be upheld [1]. It is hard to cut titanium parts from cutting tool during machining because of properties like small thermal conductivity, low modulus of elasticity and high chemical reactivity. These unique properties categorize titanium alloys into difficult-to-machine materials. Metal cutting process is not just to outline machined components yet in addition to fabricate them with the goal that they can accomplish their capacities as indicated by geometric, dimensional and surface contemplations. In manufacturing, the finishing look of the surface is adopted as the finger print of the machining process [2].

In today's competitive world, surfaces of industrial parts need to be stated in light of their function and application environment. Surface properties considerably affect friction, wear, fatigue, corrosion, thermal conductivity, etc. The group of factors [3] that affect surface roughness is shown in Figure 1. The investigation of surface is usually referred to as Surface Metrology. It implicates the evaluation of surfaces and their link to the manufacturing process that created the part and functional performance measures of the component. In order to guarantee the manufactured parts, conform to specified standards, an essential surface quality control inspection

process is carried out. This type of inspection is generally done with the stylus instrument for an extensive period of time in the manufacturing industry [4] and widely recognized. Yet, this traditional technique is a contact type measurement. Therefore, this technique is tedious and hence, not appropriate for rapid and high volume manufacturing systems. The main drawback with this contact technique is that it restricts the measuring speed. Another drawback is the resolution and precision of the stylus device that depends predominantly on the tip of the probe diameter. Stylus devices are not flexible enough to measure different geometrical parts [5]. Besides, the evaluation speed is also very slow. Machine vision systems usually utilize a camera, frame grabber, digitizer and processor for inspecting assignments. Surface roughness is characterized by using the histograms of the surface images. This vision based measurement is more reliable as it traces the surface roughness in two dimensions.

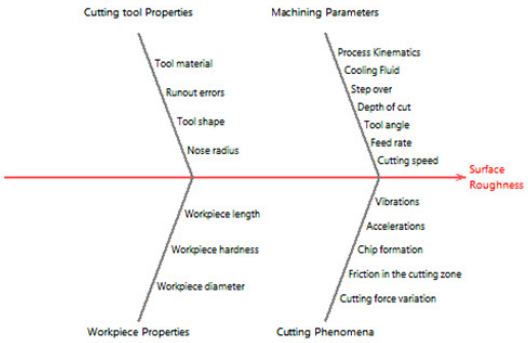

Figure 1. Fishbone Diagram Showing Parameters that affect Surface Roughness

Numerous examinations have been done to estimate the surface roughness by means of non-contact techniques. Al-Kindi et al. [6] established a texture model using the 3D data arrays from the machine vision system and found that an additional control can be obtained from the parameters based on both amplitude and space features for inspecting the manufactured parts in a machining environment. Surface roughness has been depicted with the help of the histograms of the machined surface image [7]. The authors interrelated the derived statistical parameters with the measured stylus data. Hoy and Yu [8] assessed the surface finish using the intensity histogram method and the two-dimensional (2D) Fast Fourier Transform (FFT) method. Both these methods are software driven and require large computational time. M. Gupta et al. [9] utilized the scatter spectrum of laser light replicated from the machined surfaces in his inexpensive vision system. The authors computed the various vision parameters such as standard deviation, arithmetic mean along with root mean square (RMS) values of the gray level distribution. They realized that the spindle speed and ambient lighting do not have noticeable influence on the vision parameters. J. Valíček et al [10] proposed the optical diagnostics technique to ascertain the local radii of curvature of the surface profile. The authors found a good correlation between the optically determined parameters from the proposed optical diagnostics method and those of surface standard values.

Funda Kahraman progressed a quadratic model for evaluating surface roughness in turning process of AISI 4140 steel by means of Response Surface Methodology (RSM) [11]. I.A. Choudhury et al. [12] evolved models for surface roughness assessment in turning process of EN 24T steel by means of RSM coupled with factorial design of experiments. Arunkumar M Bongale et al. [13] built an extremely effective and trained artificial neural network (ANN) model to envisage the wear rate of the Al/SiCnp/E-glass fibre hybrid composite material under various testing situations. The authors optimized the composite material used by applying the regression analysis and genetic algorithm. Pal and Chakraborty [14] suggested back propagation neural network (BPNN) model for the assessment of surface roughness in turning operation. Priya and Ramamoorthy [15] used computer vision approach for assessing the surface quality of products that are kept inclined at altering angles to the horizontal. ANN has been trained and tested by the authors to predict the roughness values, which are found to have high correlation with the traditional stylus values. The authors also applied a shadow removal algorithm to remove the shadow appearing in the digital image of the components that are set aside intentionally inclined at altering angles. Shahabi and Ratnam [16] applied both ANN and RSM models for the evaluation of surface roughness in turning operation. They determined the surface quality of products obtained through turning. U.

Natarajan et al. [17] assessed the surface quality in turning by correlating three diverse models of surface finish depiction from neural based approaches such as BPNN, differential evolution algorithm (DEA) based ANN and adaptive neuro-fuzzy inference system (ANFIS). The obtained roughness values from the three dissimilar models are in decent convention with the experimental values. D. Rajeev et al. [18] developed a real time tool wear approximation system using ANN, which provided pretty acceptable results. S. Ramesh et al [19] progressed surface roughness model on the machining of titanium alloy using RSM to assess the effect of operating parameters. R. Soundararajan et al. [20] produced A413 alloy through squeeze casting route and machined by using wire-cut electrical discharge machining process. The authors conducted multi objective optimization of wire-cut electrical discharge machining process parameters on surface roughness and metal removal rate using RSM technique. Nabeel H. Alharthi et al. [21] developed BPNN model and multivariable regression analysis to predict the surface roughness in face milling of AZ61 magnesium alloy. The authors tested the prediction model on the validation experimental set and observed that the coefficient of determination for the multivariable regression analysis and finest neural network model was found to be 93.63% and 94.93% respectively. Salah Al-Zubaidi et al. [22] applied ANFIS for the intent of prophesying the surface roughness when end milling Ti6Al4V alloy with coated and uncoated cutting tools under dry cutting conditions. The authors displayed the results that show a good agreement between the experimental and predicated values. K. Simunovic et al. [23] developed a regression model that provides a very good fit and can be used to predict roughness of face milled aluminium alloy throughout the experimental region. The authors also enacted numerical optimization reckoning two goals of minimum propagation of error and minimum roughness simultaneously throughout the region of experimentation.

Interpolation is the process of evaluating the intermediate values of a continuous event from discrete samples [24]. Image interpolation occurs when it is resized or remapped from one pixel grid to another. It directs the difficulty of propagating a high-resolution image from its low-resolution version. Image resizing is essential in order to increase or decrease the total number of pixels, whereas remapping can occur under a broader variety of circumstances: correcting for lens distortion, changing perspective, and rotating an image. Interpolation has a significant application in digital image processing to enlarge or shrink images and to revise spatial distortions. These schemes are generally used in magnification of digital images. Keys [24] derived a one-dimensional interpolation function with appropriate boundary conditions and constraints imposed on the interpolation kernel. The authors proved that the order of accuracy of the cubic convolution technique stuck between linear interpolation and cubic splines. In contrast to cubic convolution, the cubic spline technique engenders an improved high resolution sort of an image, but it is much more cumbersome to compute. Li and Orchard [25] proposed a novel noniterative orientation edge-directed interpolation algorithm for natural-image sources. The image intensity field progresses very slowly along the edge orientation than across the edge orientation. The authors demonstrated that new edge-directed interpolation has substantial enhancements over linear interpolation on optical quality of the interpolated images. Biancardi et al. [26] exploited a new magnifying detail-preserving technique to evaluate missing frequencies from the original low resolution image and to synthesize them in the high resolution image. This technique, takes benefit of sub-pixel edge estimation and consequent polynomial interpolation to yield an apparent high quality in the high resolution image.

The proposed measurement system utilizes computer vision approach for assessing the surface quality of the appropriately illumined ground surfaces. An effort is taken to digitally magnify the surface image. A comparative study has been performed with the mechanical stylus parameters in order to examine the quantification parameters evaluated. The accuracy of this digital magnification model suggests that it has the capability to assess the surface roughness very well.

2. Materials and methods

The work material used in this study is a widely used titanium alloy. It accounts for half of the total utilization of titanium around the globe. It features good machinability and exceptional mechanical properties. This “workhorse” material has very high tensile strength and toughness. Biocompatibility of Ti 6Al-4V is exceptional, specially when direct contact with tissue or bone is needed. Titanium alloy workpiece specimens of size 100 mm x 50 mm are used in the study. The compositions of the alloys (in wt. %) are given in Table 1.

Several experiments over a varied range of operating conditions are conducted in a precision surface-grinding machine for grinding Ti-6Al-4V bars. Twenty-seven grounds

Table 1. Chemical Composition of Titanium Alloy (Ti-6Al-4V)

Chemical Composition (% weight)								
Al	***V***	***Fe***	***O***	***C***	***N***	***H***	***Y***	***Ti***
6.1	4	0.16	0.11	0.02	0.01	0.001	0.001	Bal

specimens are prepared for various sets of operating conditions to acquire different surface roughness values. Operating parameters, the cutting speed (V) in the range of 1500-1900 rpm, the feed rate (f) in the range of 0.06-0.1 mm per revolution and the depth of cut (d) in the range of 0.05-0.15 mm were the process parameters considered in this study. Table 2 shows the three process parameters and three levels of the machining parameters designed in the experiments. The experiments are conducted by using Taguchi's orthogonal array [27]. The array selected for conducting the experiments is L27 (3^{13}) orthogonal array, which is having 27 rows corresponding to the number of experiments and can accommodate up to 13 variables in 13 columns and requires 26 degrees of freedom (DoF). The number of levels used for conducting experiments is 3. The experiments were designed using a Taguchi experimental design of L27 orthogonal array with three columns and twenty-seven rows. The most suitable orthogonal array L27 (2^1 x 3^2) shown in Table 3 was used for conducting the experiments.

Table 2. Machining Conditions and their Levels

Parameters	Symbol	Actual value		
		Level 1	Level 2	Level 3
Cutting speed (v), rpm	A	1500	1700	1900
Feed (f), mm/rev	B	0.06	0.08	0.1
Depth of cut (d), mm	C	0.05	0.1	0.15

Table 3. Full Factorial Design with Orthogonal Array of Taguchi L27

Experiment No.	Factor A	Factor B	Factor C
1	1	1	1
2	1	1	2
3	1	1	3
4	1	2	1
5	1	2	2
6	1	2	3
7	1	3	1
8	1	3	2
9	1	3	3
10	2	1	1
11	2	1	2
12	2	1	3
13	2	2	1
14	2	2	2
15	2	2	3
16	2	3	1
17	2	3	2

18	2	3	3
19	3	1	1
20	3	1	2
21	3	1	3
22	3	2	1
23	3	2	2
24	3	2	3
25	3	3	1
26	3	3	2
27	3	3	3

The present study uses the average surface roughness R_a, which is used most extensively in industry. It is the arithmetic absolute average value of the heights of roughness variabilities measured from the center line within the measuring length as given in Eq. (1).

$$R_a = \frac{1}{n}\sum_{i=1}^{n}|y_i| \qquad (1)$$

where y_i is the height of roughness variabilities from the mean value and n is the number of sampling data. The surface roughness of the ground Ti-6Al-4V bars is assessed with a SJ-210 portable Surface Roughness Measuring Tester, whose characteristics are given in Table 4.

Table 4. Characteristics of Surface Roughness Measuring Tester

Measurement range	360 µm
Measuring force	4 mN
Stylus material	Diamond
Tip radius	5 µm
Traversal speed	0.25, 0.5, 0.75 mm/s (Measurement) 1 mm/s (Return)
Measuring range / resolution	25 µm / 0.002 µm

The investigational set-up comprises of a vision system (CCD camera: Blue Cougar – X125Ag Matrix Vision) and an appropriate Axial Diffuse Illuminator lighting arrangement. This set-up is shown in Figure 2. The specimen is mounted on the worktable and the light source is arranged in such a way that the illumination should be uniform. A distance of approximately 20 cm is maintained between the workpiece and the camera throughout the experimental study. The captured image using a digital camera is saved with an image resolution of 2448 × 2050 pixels. The machine vision system comprises a charge coupled device(CCD) camera, lighting arrangement, image processing software, a personal computer(PC) and a video screen. The machined ground surfaces of the prepared specimens were grabbed by the CCD camera. The specimens were positioned on a flat surface and the images were grabbed. The grabbed images of the ground specimens are digitized by the frame grabber card. The digital images were then transferred from the temporarily stored frame buffer to the display monitor of the PC. The schematic layout of computer vision system for inspecting surface roughness is shown in Figure 3.

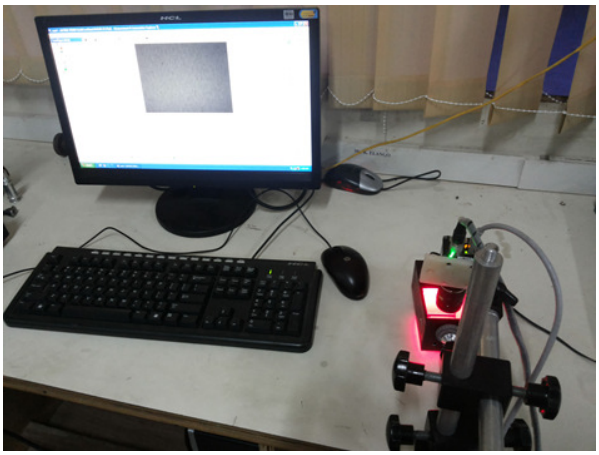

Figure 2. Experimental Setup for Inspecting Surface Roughness

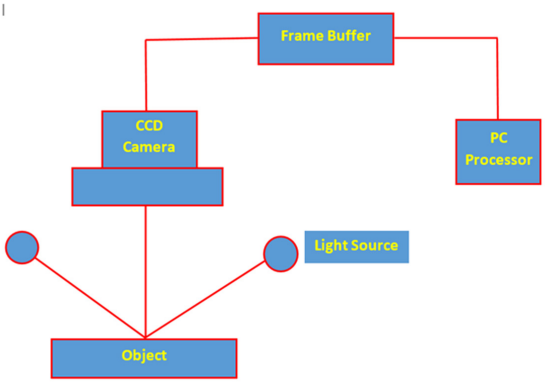

Figure 3. Schematic Layout of Computer Vision System for inspecting Surface Roughness

3. Magnification of Digital Images

Magnification of digital images is fundamentally a problem of brightness interpolation in the low resolution input image. It begins with the geometric transformation of the input pixels which are mapped to a new position in the output image. A geometric transform is a vector function T that plots the pixel (x, y) to a new position (x', y'). T is defined by its two component equations:

$$x' = T_x(x,y), \; y' = T_y(x,y) \qquad (2)$$

Equation (2) has been assumed to be planar transformation and new co-ordinate point (x', y') is obtained. The brightness interpolation of adjacent non-integer samplings provides each pixel value in the output image raster. The co-ordinates of the point (x, y) in the original image can be acquired by inverting the planar transformation in (2) in order to calculate the brightness value of the pixel (x', y') in the output image.

$$(x,y) = T^{-1}(x',y') \qquad (3)$$

The brightness is not identified since the real co-ordinates after inverse transformation do not tally the input image discrete raster. The sampled version $g_s(l\Delta x, k\Delta y)$ of the originally continuous image function f(x, y) is the only data available. The input image is resampled to get the brightness value of the point (x, y). Let the result of

the brightness interpolation be denoted by $f_n(x, y)$, where n discriminates various interpolation methods. The brightness can be uttered by the convolution equation:

$$f_n(x,y) = \sum_{l=-\infty}^{\infty} \sum_{k=-\infty}^{\infty} g_s(l\Delta x, k\Delta y) h_n(x - l\Delta x, y - k\Delta y) \quad (4)$$

The function h_n is called the interpolation kernel and it is described in a different way for different interpolation schemes. It signifies the neighborhood of the point at which brightness is preferred. Generally, only a small neighborhood is used, outside which h_m is zero. Hence, the resampling of input image produces the high resolution version of the input image and is defined as brightness interpolation. Nearest neighbor interpolation, Bilinear interpolation and Bicubic interpolation are the widely used interpolation methods for digital image magnification. Nearest neighbor interpolation algorithm is the most basic one, which needs the minimum processing time of all the interpolation methods, since it only considers one pixel that is closest to the interpolated point. Consequently, this results in making each pixel bigger. Bilinear interpolation considers the closest 2x2 neighborhood of known pixel values surrounding the unknown pixel. It then takes a weighted average of these 4 pixels to arrive at its final interpolated value. This results in much smoother looking images than nearest neighbor. In contrast to bilinear algorithm, Bicubic interpolation method considers the closest 4x4 neighborhood of known pixels that result to the total of 16 pixels. Since these are at various distances from the unknown pixel, closer pixels are given a higher weighting in the calculation. Bicubic interpolation method produces noticeably sharper images than the other two methods and also provides the ideal combination of processing time and output quality. Exhaustive treatment of concepts and mathematical description for these interpolation techniques are originally proposed by Keys [24].

4. Surface Roughness Assessment Strategy

In this work, the arithmetic average of the grey level G_a is applied to calculate the actual surface roughness of the specimen. The arithmetic average of the grey level G_a can be expressed as

$$G_a = \frac{1}{n} \sum_{i=1}^{n} |y_i| \quad (5)$$

where g_i is the difference between the grey level intensity of individual pixels in the surface image and the mean grey value of all the pixels under consideration. The grey level average (G_a) has been calculated for all the surfaces of the prepared ground specimens after capturing the images of the surfaces.

Exhaustive assessment on roughness of surfaces using image processing [28] are carried out by linking the spectra of such surfaces to the roughness values. The correlation has been shown to follow power law behavior. Extensive details of roughness emerge and appear similar to the original profile when magnified. The proposed measurement system correlates the grey level average (G_a) values attained from the images with their respective roughness values obtained from the surface roughness tester and examine the behavior of such a correlation at several degrees of image magnification for the three different interpolation techniques.

Subsequently, the captured images of workpiece specimens were magnified by factors 2, 4, 8 and 16 using the three different interpolation techniques. A correlation between G_a and surface roughness R_a was formed on the basis of data specified in Tables 5-7 (for three different interpolation techniques). A graph as shown in Figure 4 was plotted between the magnification factor and the acquired values of correlation coefficient for three different interpolation techniques.

Table 5. Variation of G_a with Varying Magnification Factors by Nearest Neighbor Interpolation

G_a (1X)	G_a (2X)	G_a (4X)	G_a (8X)	G_a (16X)	R_a (µm)
12.2012	16.0923	16.0923	16.0924	16.0925	0.287
12.7121	16.5662	16.5663	16.5663	16.5664	0.2933
10.6106	15.8834	15.8835	15.8836	15.8836	0.317

12.3458	17.1656	17.1656	17.1657	17.1658	0.346
13.1767	17.5976	17.5977	17.5978	17.5978	0.373
13.4173	19.5411	19.5411	19.5412	19.5413	0.497
13.8163	19.1595	19.1596	19.1597	19.1597	0.529
13.4183	18.7185	18.7185	18.7185	18.7185	0.772
13.8536	19.1386	19.1387	19.1388	19.1389	1.046
14.5031	19.6059	19.606	19.606	19.6061	1.105
17.0558	21.5734	21.5734	21.5735	21.5735	1.314

Table 6. Variation of G_a with Varying Magnification Factors by Bilinear Interpolation

G_a (1X)	G_a (2X)	G_a (4X)	G_a (8X)	G_a (16X)	R_a (µm)
12.2012	14.7133	14.9315	14.9503	14.9801	0.287
12.7121	15.0824	15.2845	15.3012	15.3087	0.2933
10.6106	14.4423	14.6107	14.9024	14.9168	0.317
12.3458	15.8521	15.9294	15.9491	15.9848	0.346
13.1767	16.4672	16.5567	16.5796	16.5899	0.373
13.4173	17.5615	17.7188	17.7381	17.7719	0.497
13.8163	17.5445	17.6724	17.7044	17.7194	0.529
13.4183	16.5878	16.8493	16.8893	16.8902	0.772
13.8536	17.8548	18.0221	18.1053	18.1072	1.046
14.5031	17.5865	17.7458	17.7863	17.7891	1.105
17.0558	19.2441	19.521	19.5648	19.5662	1.314

Table 7. Variation of G_a with Varying Magnification Factors by Bicubic Interpolation

G_a (1X)	G_a (2X)	G_a (4X)	G_a (8X)	G_a (16X)	R_a (µm)
12.2012	15.2537	15.3982	15.4695	15.4699	0.287
12.7121	16.0192	16.1825	16.1835	16.1835	0.2933
10.6106	15.0193	15.281	15.3286	15.3295	0.317
12.3458	16.2643	16.4641	16.4651	16.465	0.346
13.1767	17.2194	17.3024	17.3088	17.3087	0.373
13.4173	18.8761	18.8842	18.8951	18.895	0.497
13.8163	18.5999	18.6188	18.6192	18.6191	0.529
13.4183	18.0251	18.0463	18.047	18.0481	0.772
13.8536	18.8017	18.8312	18.85	18.8571	1.046
14.5031	18.8917	18.9255	18.9361	18.9372	1.105
17.0558	20.8013	20.8286	20.839	20.8411	1.314

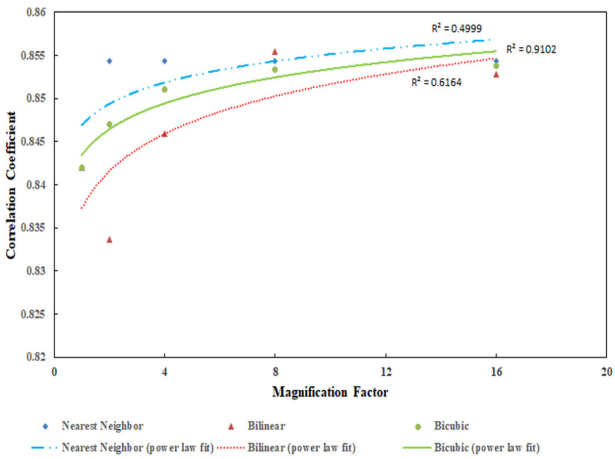

Figure 4. Variation of Correlation Coefficient with Magnification Factor for Three Interpolation Algorithms

5. Regression Analysis of Surface Roughness

Regression analyses are employed for modeling and analyzing numerous variables where there is correlation between a dependent variable and one or more independent variables [29]. In this work, the dependent variable is surface roughness (R_a), while the independent variables are cutting speed (V), feed rate (f) and depth of cut (d). Regression analysis was done to develop the predictive equation for the surface roughness. The predictive equation which was obtained by the linear regression model of surface roughness was given below.

$$R_a = -1.163 + 0.000290\ speed + 11.22\ feed + 3.347\ doc + 0.0002\ G_a$$

R-Sq(R^2) = 93.48% R-Sq(adj) = 92.29%

R-Sq is correlation coefficient and should be between 0.8 and 1 in multiple linear regression analyses [30]. It affords a correlation between the experimental and predicted results. The above models are determined to assess surface roughness within the limits of machining parameters in this study.

6. Results and Discussion

The digital images of machined work pieces have been magnified for a broad range of magnification index varying from 2X to 16X based on the three different interpolation algorithms.

Cubic convolution remains as one of the best methods for magnification of digital images in terms of preserving edge details when compared to other methods, the blurring of edges has been found to be reduced substantially [24]. Effective preservation of edges is essential for all image-processing applications including surface roughness determination. The computational simplicity offered by cubic convolution method cannot be abandoned for the slightly better result given by cubic spline method. Basically the accuracy of the interpolation technique to provide image magnification depends on its convergence rate. Cubic convolution interpolation algorithm [24] offers a O(h3) convergence rate, while cubic spline has a fourth order convergence rate, i.e. O(h4). Higher convergence rate can be achieved by altering the conditions on interpolation kernel, which in turn demands higher computational effort to derive interpolation coefficients. So there is a tradeoff between accuracy offered by an interpolation technique and efficiency in terms of computational effort it requires. Moreover, it is implemented quite easily by modern digital computers and image processors. The present algorithm is the optimal choice, although it cannot prevent the perceptible degradation of edges fully. Some amount of blurring can be seen in every magnified image.

Comparison results prove that predicted values for each response are close to experimentally measured values. The absolute error from the developed regression equations for surface roughness is found to be 6.52%. Results from the mathematical models indicate that they can be successfully applicable for predicting the surface roughness.

As mentioned earlier, owing to simplicity and limitations in the case of Nearest neighbor and Bilinear interpolation methods, magnification algorithm becomes increasingly ineffective with magnification index. This in turn means that magnified images of ground surfaces in case of Nearest neighbor and Bilinear interpolation methods, cannot predict the actual or 'true' surface characteristics of a very small region of the image (which is subject to magnification), as compared to the Bicubic interpolation algorithm, since large and irregular surface feature variation renders it difficult for the magnification algorithms to interpolate the brightness value of a pixel from that of its adjacent pixels correctly. While Bicubic interpolation method produces noticeably sharper images than the previous two methods, and perhaps the ideal combination of processing time and output quality helps magnification scheme to predict values which are remarkably closer to the actual ones. It has also been observed that the plots in Figure 4 follow the power law.

7. Conclusion

The present work clearly indicates that the Machine vision approach can be used to evaluate the surface roughness of machined surfaces. Multiple regression analysis is done to indicate the fitness of experimental measurements. Regression models obtained from the surface roughness ($R^2 > 0.93$) measurements match very

well with the experimental data. Cubic convolution interpolation method proved to be the optimal choice for magnification of digital images. The calculation of G_a, optical roughness value, from these magnified and improved images of the cubic convolution algorithm had a better correlation with the average surface roughness (R_a) measured for the ground components, when compared to other two methods. It can also be inferred that this Cubic convolution algorithm provides a better O(h3) convergence rate scheme of optical roughness estimation, indicating its effectiveness in application to the measurement using machine vision system.

References

[1] *E. O. Ezugwu and Z. M. Wang, "Titanium alloys and their machinability—a review", Journal of Materials Processing Technology, vol. 68,* ***(1997)****, pp. 262–274.*

[2] *H. Y. Kim, Y. F. Shen and J. H. Ahn, "Development of a Surface Roughness Measurement system using Reflected Laser beam", Journal of Material Processing Technology, vol. 130-131,* ***(2002),*** *pp. 662-667.*

[3] *P. Benardos and G. C. Vosniakos, "Predicting surface roughness in machining: a review", International Journal of Machine Tools and Manufacture, vol. 43, no. 8,* ***(2003),*** *pp. 833–844.*

[4] *T. R. Thomas, "Rough Surface", Imperial College Press, London,* ***(1999)****.*

[5] *B. Y. Lee and Y. S. Tarng, "Surface roughness inspection by computer vision in turning operations", International Journal of Machine Tools and Manufacture, vol. 41,* ***(2001),*** *pp. 1251–1263.*

[6] *G. A. Al-Kindi, R. M. Baul and K. F. Gill, "An application of machine vision in the automated inspection of engineering surfaces", International Journal of Production Research, vol. 30, no. 2,* ***(1992),*** *pp. 241-253.*

[7] *F. Luk, V. Huynh and W. North, "Measurement of surface roughness by a machine vision system", Journal of Physics E Scientific Instruments, vol. 22,* ***(1989),*** *pp. 977-980.*

[8] *Dep. Hoy & F. Yu, "Surface quality assessment using computer vision methods", Journal of Materials Processing Technology, vol. 28,* ***(1991),*** *pp. 265–274.*

[9] *M. Gupta and S. Raman, "Machine vision assisted characterization of machined surfaces", International Journal of Production Research, vol. 39, no. 4,* ***(2001),*** *pp. 759–784.*

[10] *J. Valíček, M. Držík, T. Hryniewicz, M. Harničárová, K. Rokosz, M. Kušnerová, K. Barčová and D. Bražina, "Non-Contact Method for Surface Roughness Measurement after Machining", Measurement Science Review, vol. 12, no. 5,* ***(2012),*** *pp. 184-188.*

[11] *Funda Kahraman, "The use of response surface methodology for prediction and analysis of surface roughness of AISI 4140 steel", Materials and Technology, vol. 43, no. 5,* ***(2009),*** *pp. 267-270.*

[12] *I. A. Choudhury and M. A. El-Baradie, "Surface roughness in the turning of high-strength steel by factorial design of experiments", Journal of Material Processing Technology, vol. 67,* ***(1997),*** *pp. 55–61.*

[13] *Arunkumar M Bongale, Satish Kumar, T. S. Sachit and Priya Jadhav, "Wear rate optimization of Al/SiCnp/E-glass fibre hybrid metal matrix composites using Taguchi method and genetic algorithm and development of wear model using artificial neural networks", Materials Research Express, vol. 5 no. 3,* ***(2018),*** *035005.*

[14] *S. K. Pal and D. Chakraborty, "Surface roughness prediction in turning using artificial neural network", Neural Computer Applications, vol. 14, no. 1,* ***(2005),*** *pp. 319–324.*

[15] *P. Priya and B. Ramamoorthy, "The Influence of Component Inclination on Surface Finish Evaluation Using Digital Image Processing", International Journal of Machine Tools and Manufacture, vol. 47, no. 3–4,* ***(2007),*** *pp. 570–579.*

[16] *H. H. Shahabi and M. M. Ratnam, "Prediction of surface roughness and dimensional deviation of workpiece in turning: a machine vision approach", International Journal of Advanced Manufacturing Technology, vol. 48,* ***(2010),*** *pp. 213–226.*

[17] *U. Natarajan, S. Palani, B. Anandampillai and M. Chellamalai, "Prediction and comparison of surface roughness in CNC-turning process by machine vision system using ANN-BP and ANFIS and ANN-DEA models", International Journal of Machining and Machinability of Materials, vol. 12, no. 1/2,* ***(2012),*** *pp. 154-177.*

[18] *D. Rajeev, D. Dinakaran and S. C. E. Singh, "Artificial neural network based tool wear estimation on dry hard turning processes of AISI4140 steel using coated carbide tool", Bulletin of the polish academy of sciences technical sciences, vol. 65, no. 4,* ***(2017),*** *pp. 553-559.*

[19] *S. Ramesh, L. Karunamoorthy and K. Palanikumar, "Surface Roughness Analysis in Machining of Titanium Alloy", Materials and Manufacturing Processes, vol. 23,* ***(2008),*** *pp. 174–181.*

[20] *R. Soundararajan, A. Ramesh, N. Mohanraj and N. Parthasarathi, "An investigation of material removal rate and surface roughness of squeeze casted A413 alloy on WEDM by multi response optimization using RSM", Journal of Alloys and Compounds, vol. 685,* ***(2016),*** *pp. 533-545.*

[21] *Nabeel H. Alharthi, Sedat Bingol, T. Adel Abbas, E. Adham Ragab, Ehab A. El-Danaf and Hamad F. Alharbi, "Optimizing Cutting Conditions and Prediction of Surface Roughness in Face Milling of AZ61 Using Regression Analysis and Artificial Neural Network", Advances in Materials Science and Engineering, vol. 1,* ***(2017),*** *pp. 1-8.*

[22] *Salah Al-Zubaidi, Jaharah A. Ghani and Che Hassan Che Haron, "Prediction of Surface Roughness When End Milling Ti6Al4V Alloy Using Adaptive Neuro Fuzzy Inference System", Modelling and Simulation in Engineering, vol. 1,* ***(2013),*** *pp. 1-12.*

[23] *K. Simunovic, G. Simunovic and T. Saric, "Predicting the Surface Quality of Face Milled Aluminium Alloy Using a Multiple Regression Model and Numerical Optimization", Measurement Science Review, vol. 13, no. 5,* ***(2013),*** *pp. 265-272.*

[24] *R. G. Keys, "Cubic convolution interpolation for digital image processing", IEEE transactions on Acoustics, Speech and Signal processing, vol. 29, no. 6,* ***(1981),*** *pp. 1153-1160.*

[25] *Li. Xin and Michael T. Orchard, "New Edge-Directed Interpolation", IEEE transactions on Image processing, vol. 10, no. 10,* ***(2001),*** *pp. 1521-1527.*

[26] *A. Biancardi, L. Cinque and L. Lombardi, "Improvements to image magnification", Pattern Recognition, vol. 35,* ***(2002)****, pp. 677–687.*

[27] *P. J. Ross, "Taguchi Techniques for Quality Engineering", McGraw-Hill, New York,* ***(1996)****.*

[28] *A. Majumdar and B. Bhushan, "Role of fractal geometry in roughness characterization and contact mechanics of surfaces", ASME Journal of Tribology, vol. 112,* ***(1990)****, pp. 205–216.*

[29] *M. H. Cetin, B. Ozcelik, E. Kuram and E. Demirbas, "Evaluation of vegetable based cutting fluids with extreme pressure and cutting parameters in turning of AISI 304L by Taguchi method", Journal of Cleaner Production, vol. 19,* ***(2011),*** *pp. 2049–2056.*

[30] *D. C. Montgomery, "Design and Analysis of Experiments", John Wiley & Sons Inc, OC, USA,* ***(2001)****.*